(A New Proposal to Jefferson Lab PAC-22)

Measurement of Charge Pion Production Ratios in Semi-Inclusive Deep-Inelastic Scattering at 6 GeV

F. Benmokhtar, R. Gilman, C. Glashausser, X. Jiang (Co-Spokesperson) [a] ,
G. Kumbartzki, K. McCormick, R. Ransome (Co-Spokesperson)

Rutgers University, Piscataway, New Jersey.

J.-P. Chen (Co-Spokesperson), E. Chudakov, J. Gomez, D.W. Higinbotham, O. Hansen, C. W. de Jager, M. Jones, J. LeRose, W. Melnitchouk, R. Michaels, S. Nanda, B. Reitz, A. Saha, B. Wojtsekhowski

Jefferson Lab, Newport News, Virginia.

P. Markowitz

Florida International University, Miami, Florida.

T.-H. Chang

University of Illinois , Urbana-Champaign, Illinois.

W. Korsch, P. Zolnierczuk

University of Kentucky, Lexington, Kentucky.

W. Bertozzi, O. Gayou, S. Gilad, X. Zheng, Z. Zhou

Massachusetts Institute of Technology, Cambridge, Massachusetts.

F. Butaru, Seonho Choi, Z.-E. Meziani, K. Slifer, P. Solvignon, N. Ploquin, H. Yao

Temple University, Philadelphia, Pennsylvania.

J. Calarco and W. Hersman

University of New Hampshire, Durham, New Hampshire.

A. Deur, R. Lindgren, N. Liyanage, B. Norum, K. Wang

University of Virginia, Charlottesville, Virginia.

T. Averett, K. Kramer, V. Sulkosky, X. Zhu

College of William and Mary, Williamsburg, Virginia.

V. Nelyubin

St-Petersburg Nuclear Physics Institute, Gatchina, Leningrad district, 18835, Russia.

[a] Contact person. Email: jiang@jlab.org

We propose to measure the semi-inclusive $(e, e'\pi^+)$ and $(e, e'\pi^-)$ yield ratios on hydrogen, deuterium and helium-3 targets in the deep inelastic scattering region of $0.15 < x < 0.35$ and $1.1 < Q^2 < 2.7$ (GeV/c)^2 (with $2.5 < W < 3.1$ GeV and $1.8 < W' < 2.6$ GeV) in Jefferson Lab Hall A with an incident electron beam of 6 GeV energy. The combined yield ratios of charged pions on a proton and a neutron would be independent of $z = E_\pi/\nu$ if factorization between the virtual photon-quark scattering and quark hadronization applies. We propose to determine the yield ratios to 2% statistical accuracy in order to test the level of violation of factorization at the Jefferson Lab energy scale. A total of 156 hours (6.5 days) of unpolarized beam is requested.

1 Introduction: Factorization in semi-inclusive reactions.

Semi-inclusive deep inelastic scattering (DIS) offers a great opportunity for determining the spin, flavor, and sea structure of the nucleon [1] , as well as extracting information on new distributions [2] (such as the transversity) which are not accessible in inclusive scattering, thereby significantly enriching our understanding of QCD and the nucleon structure.

At high energy the scattering and production mechanisms factorize: the cross section at leading order in QCD becomes a simple product of the structure function, which gives the probability of finding a quark in the nucleon, and a quark $\rightarrow$ meson fragmentation function, the probability that the quark hadronizes into the meson. The usefulness of semi-inclusive production lies in its ability to identify individual quark species in the nucleon by tagging specific mesons in the final state, so that both the flavor and spin of the quarks and antiquarks can be uniquely determined.

The extent to which factorization applies at lower energies is an open question. HERMES has demonstrated that, within their experimental precision, factorization works reasonably well at the HERMES kinematic conditions. Jefferson Lab is actively pursuing the opportunity of an energy upgrade to 12 GeV. Semi-inclusive processes could be a very rich program with the 12 GeV upgrade if factorization works to a reasonable level. The fact that Jefferson Lab has the highest luminosity, at the level of a few times 10^{38} particles/sec/cm^2, and 100% duty factor, would make it a unique facility to do precision semi-inclusive measurements to study the nucleon spin flavor and sea structure. The question of how well factorization will hold at the kinematics accessible with the 12 GeV upgrade is crucial for determining how clean and important the semi-inclusive program can become.

Recent Jefferson Lab Hall B results, with an incident electron energy of 4.3 GeV, of the single spin asymmetry for semi-inclusive π production show a similar behavior (at the experimental accuracy of $< 50\%$) as the HERMES results with 27.5 GeV incident energy. It is an indication that the violation of factorization might be smaller than would be naively expect even at this rather low energy. One notable point is that the incident beam energy is only one of the kinematic variables. With the high luminosity of Jefferson Lab, it is often possible to perform precision measurements at large scattering angles, which makes Q^2 and W comparable to that of HERMES.

With this in mind, the Jefferson Lab 12 GeV upgrade has great potential to open up a large DIS kinematic range for semi-inclusive measurements.

To quantitatively answer the question of factorization at Jefferson Lab energies, it is crucial to perform precision tests to quantify how well factorization holds (or how large the violation of factorization is). It is the main aim of this proposal to quantify the violation of the factorization. It is anticipated that with 6 GeV incident energy, the violation of factorization should be larger than that with 12 GeV incident energy. Therefore, the test at 6 GeV will be a more sensitive one.

Furthermore, the violation of factorization (or the approach of factorization) is by itself a very interesting topic. There is currently no clear theoretical answer as to the question of at what energy or Q^2 (or other kinematic conditions) factorization should hold. A quantitative experimental study will provide important input to the theoretical study of the semi-inclusive processes and help shed light on our understanding of the transition of QCD from the low energy to the high energy regimes.

1.1 Semi-inclusive pion production in electron scattering.

At high enough energy transfer, independent factorization is assumed between the virtual photon-quark hard scattering process and the hadronization of the struck quark. This implies:

$$Y^{\pi^\pm}(x,z) \propto \sum_i e_i^2 \left[q_i(x) D_{q_i}^{\pi^\pm}(z) + \bar{q}_i(x) D_{\bar{q}_i}^{\pi^\pm}(z) \right], \tag{1}$$

where $Y^{\pi^+}(x,z)$ ($Y^{\pi^-}(x,z)$) is the π^+ (π^-) yield in deep-inelastic scattering, $z = E_\pi/\nu$ is the fraction of the virtual photon energy carried by the pion, e_i is the quark charge, $q_i(x)$ and $\bar{q}_i(x)$ are the density distributions of the quarks and anti-quarks. The fragmentation functions $D_{q_i}^{\pi^\pm}(z)$ represent the probability that a quark of flavor i fragments into a charged pion. Assuming isospin symmetry and charge conjugation invariance, the number of light quark fragmentation functions is reduced to two types: the favored (D^+) and the unfavored (D^-) fragmentation functions:

$$D^+ \equiv D_u^{\pi^+} = D_d^{\pi^-} = D_{\bar{u}}^{\pi^-} = D_{\bar{d}}^{\pi^+}, \tag{2}$$

$$D^- \equiv D_u^{\pi^-} = D_d^{\pi^+} = D_{\bar{u}}^{\pi^+} = D_{\bar{d}}^{\pi^-}. \tag{3}$$

The HERMES collaboration published data on the ratio of $(\bar{d}-\bar{u})/(u-d)$ in the kinematic range of $0.02 < x < 0.3$ and $1 < Q^2 < 10$ GeV^2. Through measurements of the yield ratio

$$r(x,z) = \frac{Y_p^{\pi^-}(x,z) - Y_n^{\pi^-}(x,z)}{Y_p^{\pi^+}(x,z) - Y_n^{\pi^+}(x,z)}, \tag{4}$$

the flavor asymmetry was determined from:

$$\frac{\bar{d}(x)-\bar{u}(x)}{u(x)-d(x)} = \frac{J(z)[1-r(x,z)]-[1+r(x,z)]}{J(z)[1-r(x,z)]+[1+r(x,z)]}, \tag{5}$$

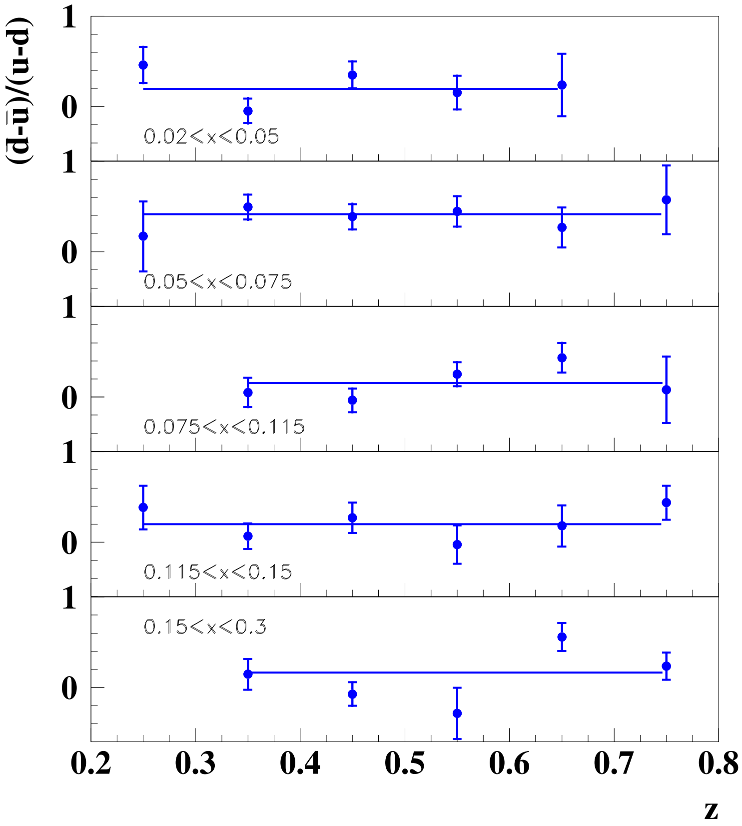

Figure 1: HERMES evidence of factorization. The extracted distribution of $(\bar{d}-\bar{u})/(u-d)$ as a function of z in five bins of x.

in which $J(z) = \frac{3}{5}\left(\frac{1+D'(z)}{1-D'(z)}\right)$ with $D'(z) = D_u^{\pi^-}/D_u^{\pi^+}$. To demonstrate factorization, HERMES measured the flavor asymmetry $(\bar{d}-\bar{u})/(u-d)$ for five x-bins as a function of z as shown in Fig. 1. Since no strong indication of z dependence was observed, the data are considered to be consistent with the assumption of factorization as in Eq. 1.

From combined yield ratios of charge pion production on the proton and deuteron, HERMES extracted $d_v(x)/u_v(x)$ as shown in Fig 2. The good agreement with QCD fit curve [4] and other high energy data served as a strong indication of factorization in the HERMES data [5].

HERMES also extracted fragmentation functions [6] from semi-inclusive data. By comparing the extracted fragmentation functions to those from the EMC data as shown in Fig 3, the HERMES results demonstrated that the fragmentation functions are universal functions independent of the reaction channels and parton distributions.

Although the HERMES data were collected at a positron beam energy of 27.5

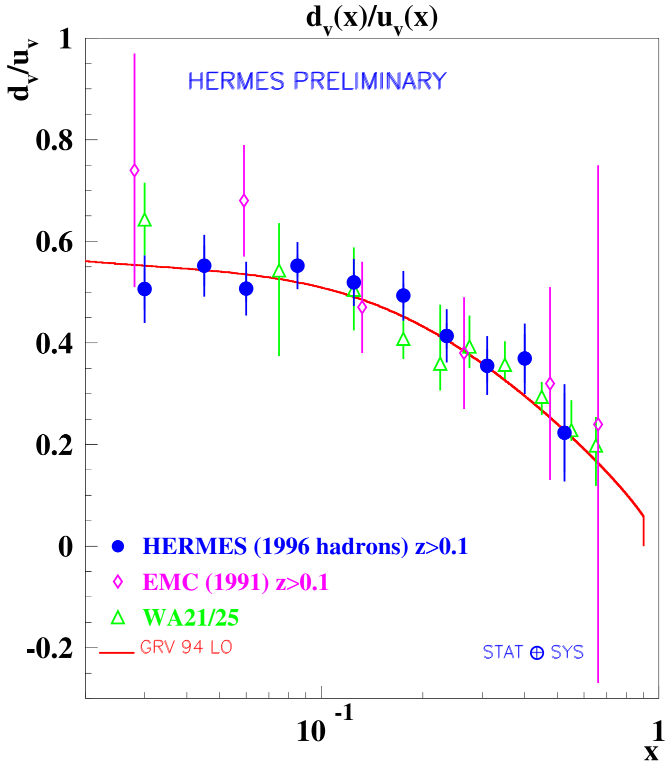

Figure 2: HERMES d_v/u_v.

GeV, we note that the evidence for factorization occurred at $1.33 < Q^2 < 4.88$ GeV^2, with the requirement that the invariant mass $W > 2.0$ GeV. At Jefferson Lab Hall A with a beam energy of 6.0 GeV, due to the much higher luminosity, scattering at larger angles becomes possible making a similar kinematic region with $1.1 < Q^2 < 2.7$ GeV^2 and $W > 2.5$ GeV accessible, as chosen in this proposal.

1.2 Observables that could indicate the onset of factorization

If an independent factorization applies between the virtual photon-quark hard scattering process and the hadronization of the struck quark, quark fragmentation functions would be canceled out in certain combinations of charged pion production ratios. The z-independent behavior of these ratios would be a clear indication of the onset of factorization.

Assuming isospin symmetry and charge conjugation (i.e. $u_p(x) = d_n(x)$, $d_p(x) = u_n(x)$, $\bar{u}_p(x) = \bar{d}_n(x)$, $\bar{d}_p(x) = \bar{u}_n(x)$) and neglecting heavy quark contributions while considering the valence region only, and under the assumption of independent factorization of Eq. 1, the semi-inclusive yield of π^+ and π^- on a proton and a free neutron can be expressed as:

$$Y_p^{\pi^+}(x,z) = A\left(4u(x)D^+(z) + d(x)D^-(z) + 4\bar{u}(x)D^-(z) + \bar{d}(x)D^+(z)\right), \quad (6)$$

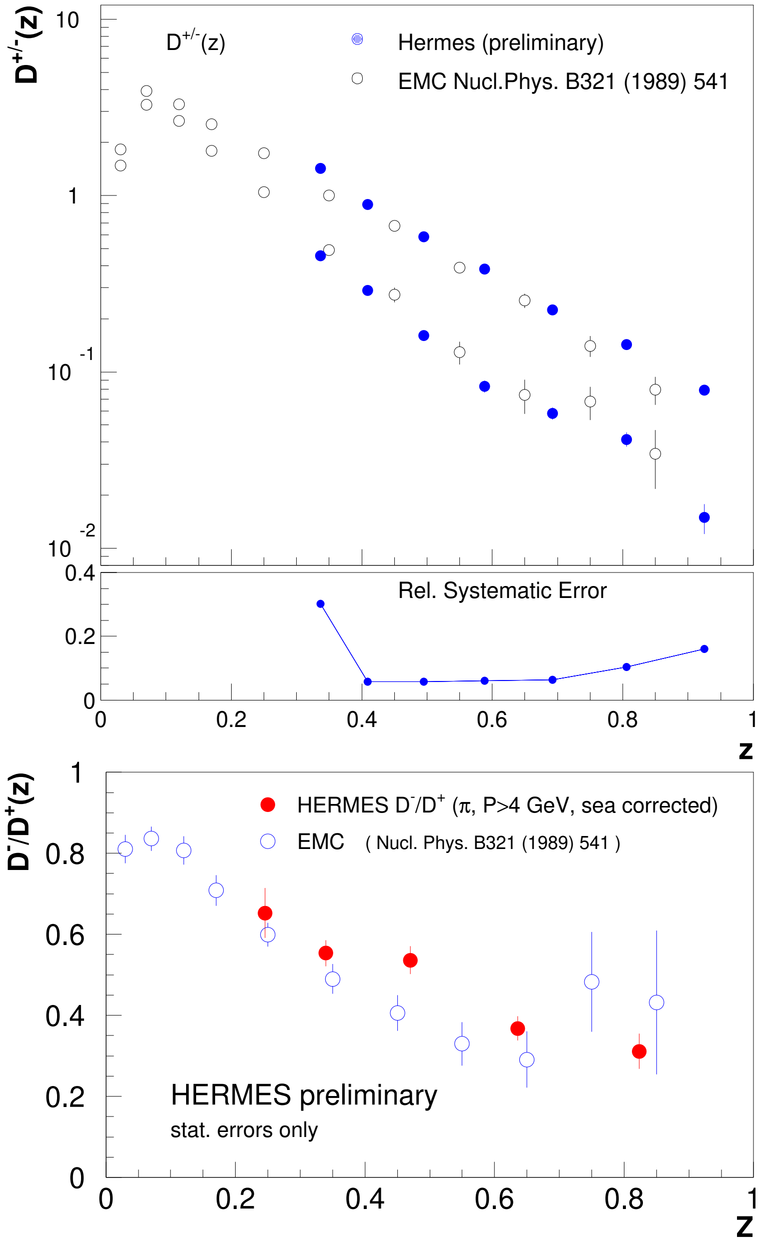

Figure 3: HERMES extracted favored and unfavored fragmentation functions is shown in the top panel in comparison to EMC data. The ratio of D^-/D^+ is shown in the bottom panel. (P. Geiger Ph.D. thesis, Ruprecht-Karls-University, Heidelberg, 1998.)

$$
\begin{aligned}
Y_p^{\pi^-}(x,z) &= A\left(4u(x)D^-(z) + d(x)D^+(z) + 4\bar{u}(x)D^+(z) + \bar{d}(x)D^-(z)\right),\\
Y_n^{\pi^+}(x,z) &= A\left(4d(x)D^+(z) + u(x)D^-(z) + 4\bar{d}(x)D^-(z) + \bar{u}(x)D^+(z)\right),\\
Y_n^{\pi^-}(x,z) &= A\left(4d(x)D^-(z) + u(x)D^+(z) + 4\bar{d}(x)D^+(z) + \bar{u}(x)D^-(z)\right).
\end{aligned}
$$

where A is a common kinematic factor, and the explicit Q^2 dependence has been left out for clarity. If four independent yields ($Y_p^{\pi^+}, Y_p^{\pi^-}, Y_n^{\pi^+}$ and $Y_n^{\pi^-}$) are determined, two yield ratios can be formed in which the fragmentation functions cancel out:

$$
t_1(x) = \frac{Y_p^{\pi^+}(x,z) + Y_p^{\pi^-}(x,z)}{Y_n^{\pi^+}(x,z) + Y_n^{\pi^-}(x,z)} = \frac{4u(x) + d(x) + 4\bar{u}(x) + \bar{d}(x)}{4d(x) + u(x) + 4\bar{d}(x) + \bar{u}(x)}, \tag{7}
$$

$$
t_2(x) = \frac{Y_p^{\pi^+}(x,z) - Y_p^{\pi^-}(x,z)}{Y_n^{\pi^+}(x,z) - Y_n^{\pi^-}(x,z)} = \frac{4u(x) - d(x) - 4\bar{u}(x) + \bar{d}(x)}{4d(x) - u(x) - 4\bar{d}(x) + \bar{u}(x)}. \tag{8}
$$

Clearly, observation of the z-scaling behavior of t_1 and t_2 would be a strong indication of factorization. We note that the independent factorization assumption of Eq. 1 is not an absolute requirement in the cancellation of the fragmentation functions in Eq. 7 and Eq. 8. A less restrictive form of factorization can be accepted in which the fragmentation functions can take a more general form. As long as the fragmentation functions do not explicitly depend on the quark distributions, the ratios t_1 and t_2 will be independent of z as a consequence of isospin symmetry and charge conjugation invariance. In such a case, the yield ratios t_1 and t_2 will be a direct measurement of the quark distribution ratios and not related to the fragmentation functions.

In this experiment, we seek to determine the semi-inclusive π^+ and π^- yield on proton, and neutron through measurements on hydrogen, deuterium and helium-3 targets with high statistical accuracy in the kinematic region of $0.11 < x < 0.34$, $1.1 < Q^2 < 2.7$ GeV^2, and $2.5 < W < 3.1$ GeV. The invariant mass of the hadron system without the detected pion will be above the resonance region with $1.8 < W' < 2.6$ GeV. Through measurements at different z, we plan to study the z-dependency of t_1 and t_2 to statistical accuracies of 2.0% in order to quantify the level of violation of factorization. We note that the exact knowledge of the fragmentation functions is not needed in this experiment.

The proton yield comes from the hydrogen data directly, while the neutron yield can be formed either from deuteron and hydrogen difference or from helium-3 and hydrogen difference. Nuclear binding effects and corrections due to Fermi motion are expected to be small [7] in the kinematic region of $0.11 < x < 0.34$ and will be applied to the data according to the best available model calculations.

To maximize the precision on t_1 and t_2 measurements one needs to obtain the yields from hydrogen, deuterium and helium-3 targets with similar relative accuracy and measure the π^+ and π^- yields with similar absolute accuracy for each target. If z scaling is found not to be strongly violated, the much higher statistical accuracy than HERMES possible at JLab will provide information on quark distributions and their polarization distributions with reasonable accuracy in semi-exclusive experiments.

2 The Experiment

We plan to study the deep inelastic $(e, e'\pi^+)$ and $(e, e'\pi^-)$ reactions at the highest possible W available at JLab with a 6 GeV beam energy. The experiment will use the Hall A left-side HRS spectrometer with the septum magnet at 6° as the hadron arm, and use the Big Bite spectrometer at 30° beam-right as the electron arm. The detector configuration of the Big Bite spectrometer will be the same as in the Hall A G_E^n experiment [8] (E02013), in which a set of lead-glass pre-shower and shower calorimeter are to be mounted at the back of the standard Big Bite detector package for e/π^- separation.

2.1 Kinematics choice

The kinematic variables are defined in Fig. 4. E′ is the energy of the scattered electron and its scattering angle is fixed at around $\theta_e = 30°$ in this experiment, $x = Q^2/(2M_N\nu)$ where $\nu = E - E'$ is the energy transfer. The momentum of the detected charge pion is p_π and z is the fraction of the energy transfer the pion carries $z = E_\pi/\nu$. W is the invariant mass of the whole hadron system and W' is the invariant mass of the hadron system without the detected pion. We chose to cover

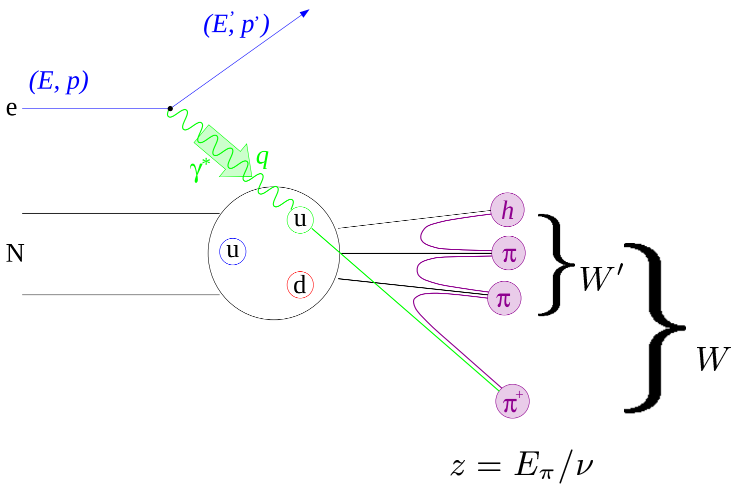

Figure 4: The (e,e'π) reaction on a nucleon and the definition of kinematic variables.

the deep inelastic region of $0.15 < x < 0.35$ and the highest possible W with 6 GeV beam. We also chose to detect the leading fragmentation products, which carries $z = 0.35 \sim 0.75$ of total energy transfer, directly along the momentum transfer $\vec{q}$ direction, to favor the current fragmentation regime. In the two-dimensional plot [9] of z vs the center of mass rapidity η_{CM}, where $\eta_{CM} = \frac{1}{2} ln \frac{E+P_L^\star}{E-P_L^\star}$ in the center of mass frame, as shown in Fig 5 for the worst case of $x = 0.34$ bin with $W = 2.5$ GeV, the rapidity gap between the two fragmentation regime is at least $\Delta\eta_{CM} = 3.5$ when

$z > 0.35$ is required, which is well above the regularly used Berger's Criterion of $\Delta\eta_{CM} = 2.0$ for separation of current and target fragmentation [10].

Detecting hadrons along $\vec{q}$ not only gives a high coincidence rate, it also limits the differences of transverse momentum (p_t) spread between different z settings such that possible complications of a strong z dependence entangled with a strong p_t dependence can be minimized.

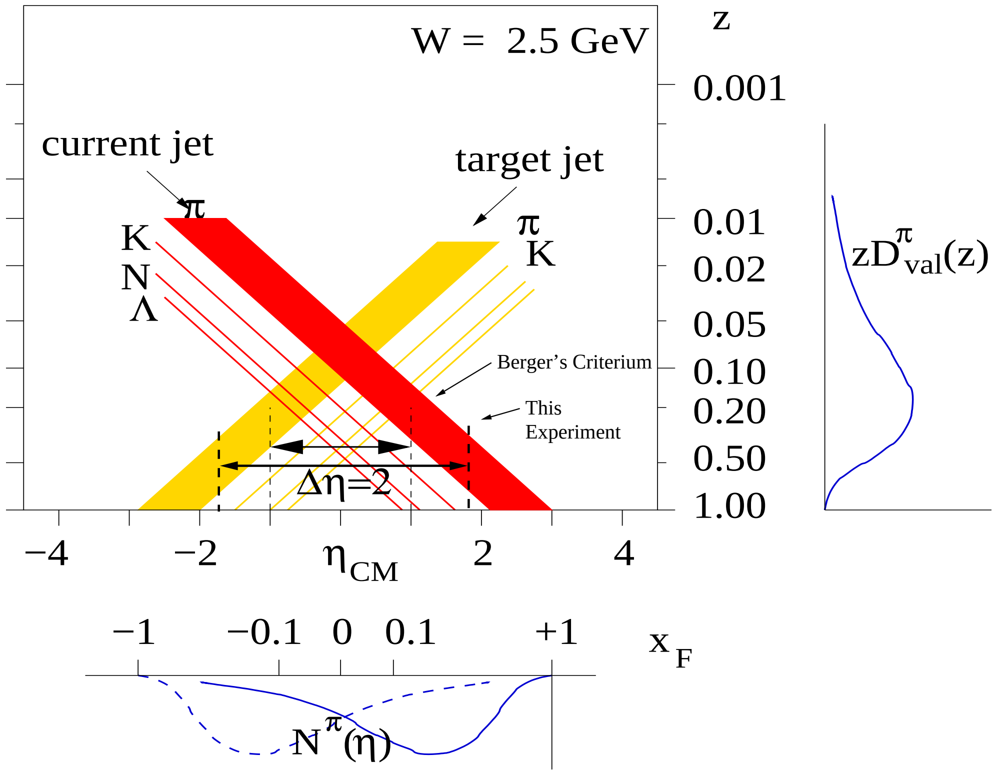

Figure 5: The center-of-mass rapidity gap for $W = 2.5$ GeV (the highest x-bin), above $z = 0.35$ the current and target fragmentation regime should be separated by $\Delta\eta_{CM} = 3.5$. A typical fragmentation function is shown on the side panel with $z = E_\pi/\nu$ and $x_F = p_L^{\pi\star}/|\vec{q}|$. From P. J. Mulders, hep-ph/0010199.

The value of W' is chosen to be as high as possible (1.8∼2.6 GeV) to avoid contributions from resonance structures. These requirements make the direction of $\vec{q}$ very close to the beam direction, thus, the use of the septum magnet is necessary to provide 6° access in order to detect leading hadrons along $\vec{q}$. Since the septum magnet shifts the interaction point 80 cm upstream of the regular interaction point, the other HRS spectrometer cannot be used to detect electrons. Instead, the Big Bite spectrometer will be used as the electron arm. The coincidence event rates of this experiment are expected to be high, so we can push back the Big Bite spectrometer to a larger drift distance (2.4 meter) in order to reduce low-energy background in the singles trigger. The central kinematic values for each 0.2 GeV E'-bin are listed in Fig. 1

Within one Big Bite setting, the finite solid angle acceptance ($\Delta\Omega$ = 36 msr at 2.4 meter drift) and large momentum bite (at least 0.6∼1.8 GeV) allow a wide kinematic region to be covered. If we take six uniform E' bins between 0.6∼1.8 GeV, the corresponding coverage in the (x, W) plane and in the (x, Q^2) plane are shown in Fig. 6.

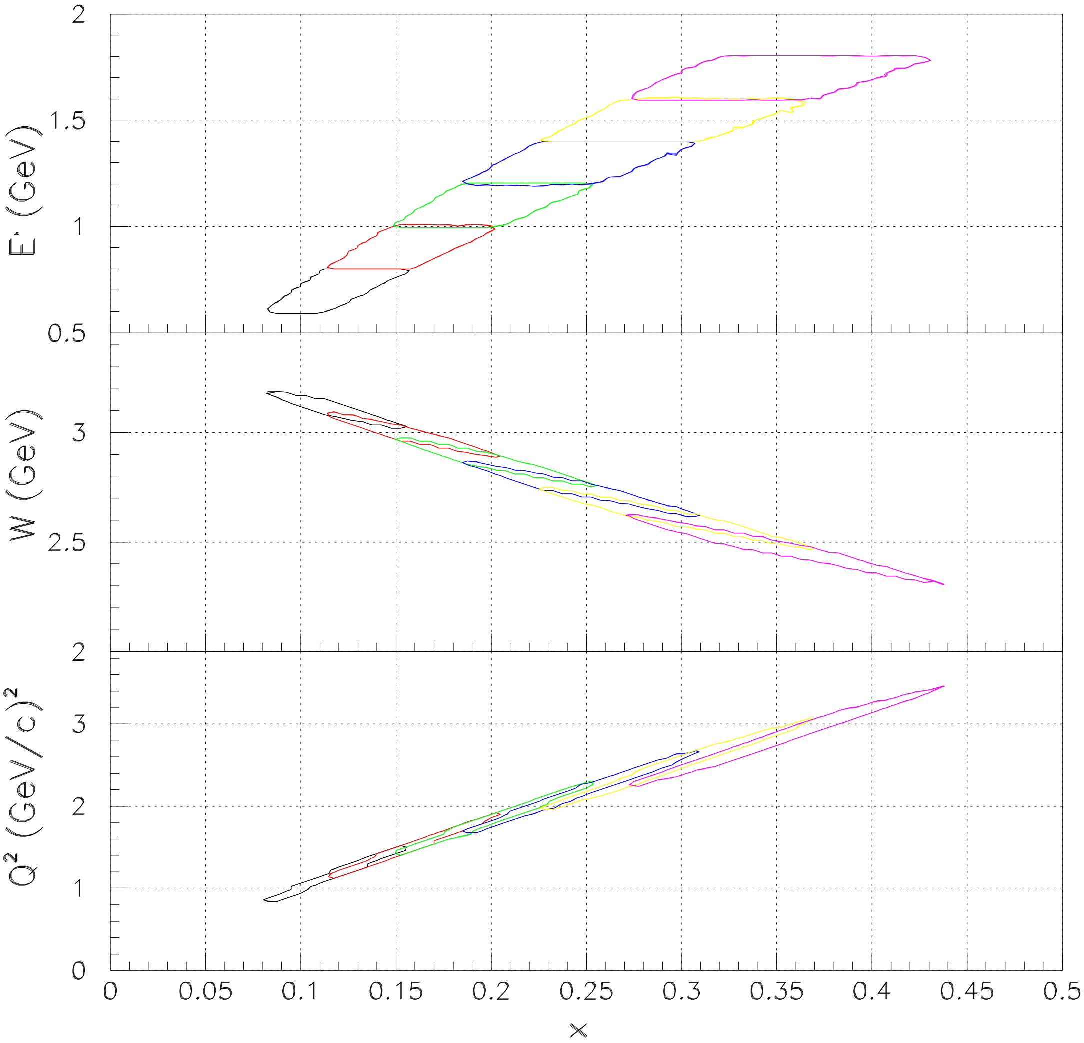

Figure 6: The phase space coverage in (x, W) plane and in (x, Q^2) plane corresponding to six bins in E' labeled by different colors.

We will take five HRS momentum settings from 1.7 to 3.7 GeV/c to cover z from 0.32 to 0.70. The available phase space in the (x, W') and (x, p_t) planes for each HRS momentum setting is shown in Fig. 7. Within each setting, several bins of E' are plotted following the same color code in Fig. 6.

The Hall-A floor configuration for this experiment has been checked with the Hall A mechanical design group to make sure no interference between different elements.

Table 1: Central kinematic values for each E'-bin. The beam energy is $E = 6.0$ GeV. Five hadron arm momentum setting will be taken. E′ (GeV) and θ_e (degree) are electron arm momentum and angle. Singles electron rates for each bin are listed for the Hydrogen target case with 5 μA of beam current. The hadron arm angle is fixed at 6°, and P_π (GeV/c) is the hadron arm momentum. W (in GeV) is the invariant mass of the hadron system, W' (in GeV) is the invariant mass of the hadron system without the detected pion.

E′	θ_e	$\langle x \rangle$	W	Q^2	$\text{Rate}_{(e,e')}$	P_π	z	W'
0.700	30.0	0.11	3.11	1.13	918.9			
						1.70	0.32	2.61
						2.20	0.42	2.45
						2.70	0.51	2.27
						3.20	0.60	2.08
						3.70	0.70	1.87
0.900	30.0	0.15	3.00	1.45	756.1			
						1.70	0.33	2.50
						2.20	0.43	2.34
						2.70	0.53	2.16
						3.20	0.63	1.97
1.100	30.0	0.19	2.88	1.77	629.8			
						1.70	0.35	2.38
						2.20	0.45	2.22
						2.70	0.55	2.04
						3.20	0.65	1.85
1.300	30.0	0.24	2.76	2.09	525.6			
						1.70	0.36	2.26
						2.20	0.47	2.10
						2.70	0.58	1.92
1.500	30.0	0.29	2.63	2.41	432.4			
						1.70	0.38	2.13
						2.20	0.49	1.97
						2.70	0.60	1.79
1.700	30.0	0.34	2.49	2.73	345.7			
						1.70	0.40	1.99
						2.20	0.51	1.83

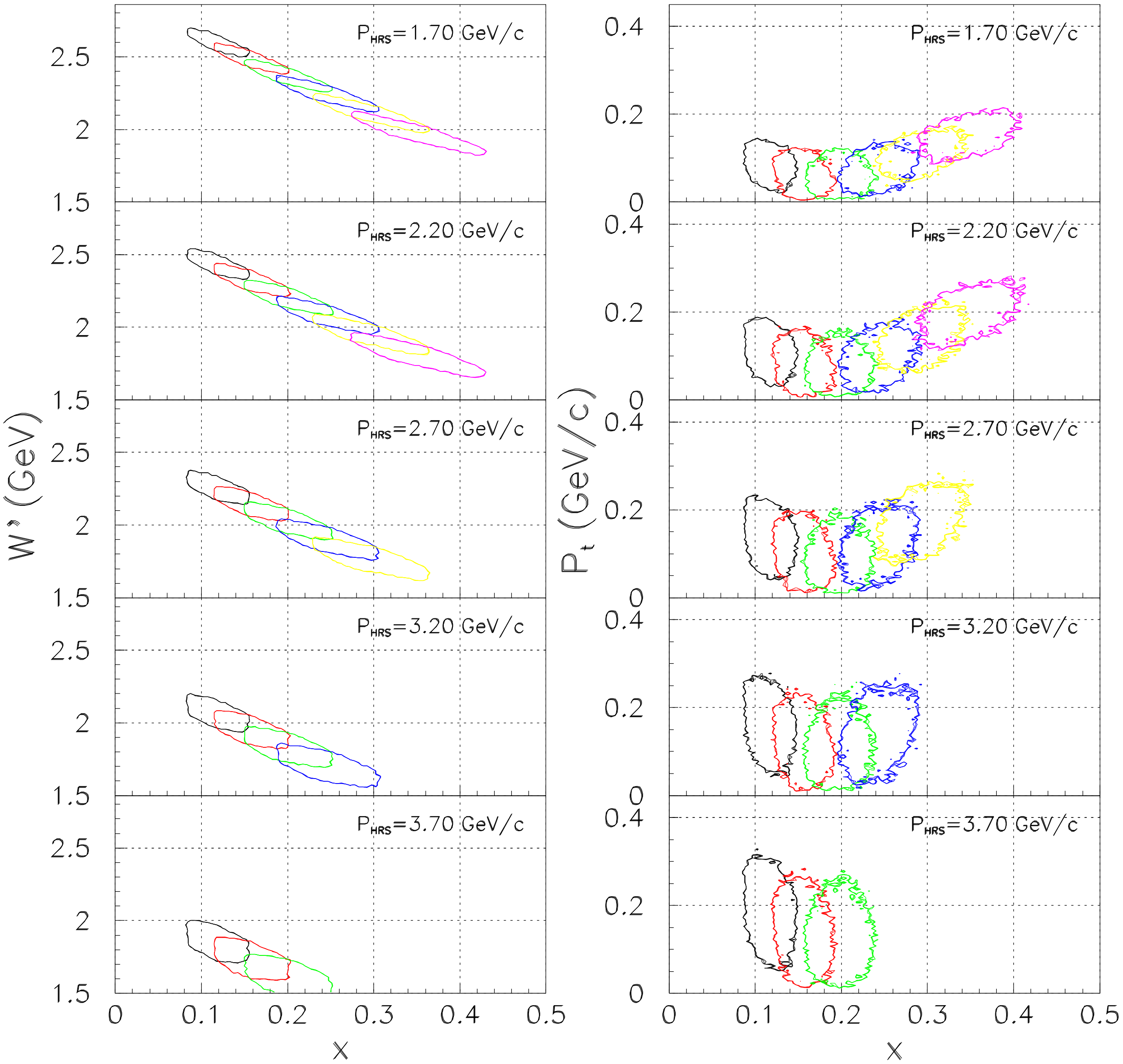

Figure 7: The phase spaces for five different HRS settings in (x, W') and (x, p_t) plane. Several bins of E' are plotted following the same color code as in the previous plots.

The Big Bite magnet will be located 2.4 meters away from the target at an angle of 30°. Well-collimated shielding is planned in front of the magnet to reduce background. Shielding between the detector package and the beam dump will also be required.

The standard 15 cm Hall A cryogenic Hydrogen and Deuterium targets will be used. The Helium-3 target loop will be operating at 20K and 250 psi pressure to ease cooling complications. Three target loops will be cooled on the same 15K cooling line. Target density will be monitored by pressure and temperature measurements. Single arm electron events will also be used to correct for target density changes.

2.2 Spectrometers and detectors

Left Side HRS Spectrometer and Detectors

The left side HRS spectrometer will be in its standard configuration with a threshold gas Cherenkov for e/π^- separation, and an aerogel Cherenkov for π^+/p separation. Two layers of lead glass shower counters at the back of the detector package will provide additional information on particle identifications.

The Electron Arm Spectrometer and Detectors

We plan to put the Big Bite spectrometer at 2.4 meters drift from the target as the electron arm. The detector package configuration will be exactly the same as in the G_E^n experiment. The following considerations were taken into account:

- To provide particle ID and good pion rejection, well segmented shower detectors should be used. A pre-shower and a shower calorimeter will be needed, as in the planned G_E^n experiment (E02013).
- Reconstruction of the vertex in target gives a large reduction factor on accidental events. Reasonable target reconstruction can be done with Big Bite which has simple optics.
- Knowledge of the electron energy with the calorimeter allows the trajectory of electron to be reconstructed even with multiple hit events in the chambers.

The detector configuration of the Big Bite spectrometer is shown in Fig 8. A GEANT Monte Carlo simulation[8] was performed to guide the design of the electron arm detector package. The expected momentum resolution in E02013 with different drift chamber position resolutions is shown in Fig. 9. Since this experiment does not seek to resolve any structures in the final states, the requirement for momentum and angular resolution is very modest. The momentum resolution designed for E02013 will be more than adequate for this proposal. The angular resolution will be about 3.0 mrad in each direction, causing only a few MeV spread in P_t reconstruction. The vertex resolution will be better than 2.0 cm (along the beam).

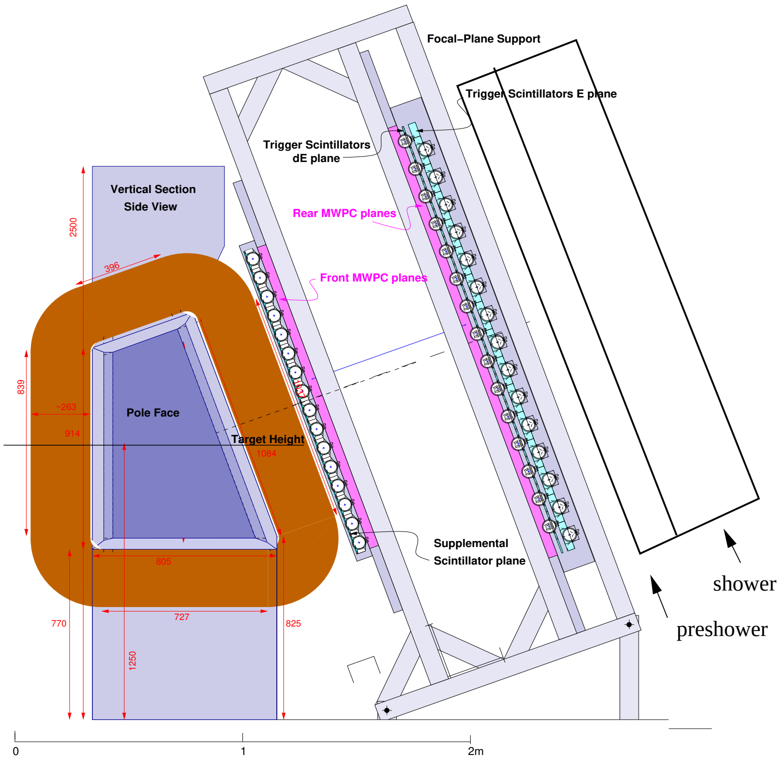

Figure 8: The side view of the Big Bite spectrometer with its detector package. The location of two wire chambers and two lead glass array are shown.

Under the above configuration, a solid angle of 36 msr can be achieved over a momentum range of 0.6 $\sim$ 1.8 GeV/c. Fig. 10 shows Monte Carlo simulation results[11] of the Big Bite momentum acceptance and the expected solid angle as a function of interaction point.

2.3 Background rates and accidental coincidence rates.

Single electron rates in each arm are estimated using deep inelastic scattering cross sections. Due to its largely open geometry and relatively weak dipole field, the Big Bite spectrometer will accept electrons with momenta starting roughly from 0.2 GeV up to the beam energy. In Table 2 the singles electron rates in each 200 MeV bin in Big Bite are listed. We assume a 5 μA beam on a 15 cm liquid hydrogen target. The single arm π^-/e^- ratio should not be more than 10:1 based on data collected in a similar kinematics during experiment E99117. Therefore, total negative charged particle rates in Big Bite should be less than 80 kHz. With the planned pre-shower and shower detector(almost the same asthe right arm HRS pre-shower and shower package in size and configuration) a pion rejection factor of 100 can be easily achieved.

Positive pion, positron, and proton rates were estimated by P. Degtiarenko's Monte Carlo simulation code GDINR [12]. The integrated rates for particles with

Table 2: Rates of single electrons in each 200 MeV bin in the Big Bite spectrometer assuming a 5 μA beam on a 15 cm liquid Hydrogen target. Single electron rates on a Deuterium or a Helium-3 target are comparable.

E'	θ_e	$\langle x \rangle$	W	Q^2	$\text{Rate}_{(e,e')}$
GeV	deg.		GeV	$(\text{GeV/c})^2$	Hz
0.300	30.0	0.03	3.35	0.48	1568.5
0.500	30.0	0.07	3.23	0.80	1150.2
0.700	30.0	0.11	3.11	1.13	918.9
0.900	30.0	0.15	3.00	1.45	756.1
1.100	30.0	0.19	2.88	1.77	629.8
1.300	30.0	0.24	2.76	2.09	525.6
1.500	30.0	0.29	2.63	2.41	432.4
1.700	30.0	0.34	2.49	2.73	345.7
1.900	30.0	0.40	2.35	3.05	264.7
2.100	30.0	0.46	2.20	3.38	190.2
2.300	30.0	0.53	2.03	3.70	124.1
2.500	30.0	0.61	1.85	4.02	69.4
2.700	30.0	0.70	1.65	4.34	29.8
2.900	30.0	0.80	1.43	4.66	7.5
...					...
Total Electron Singles Rate in Big Bite					**$\sim$ 7 kHz**

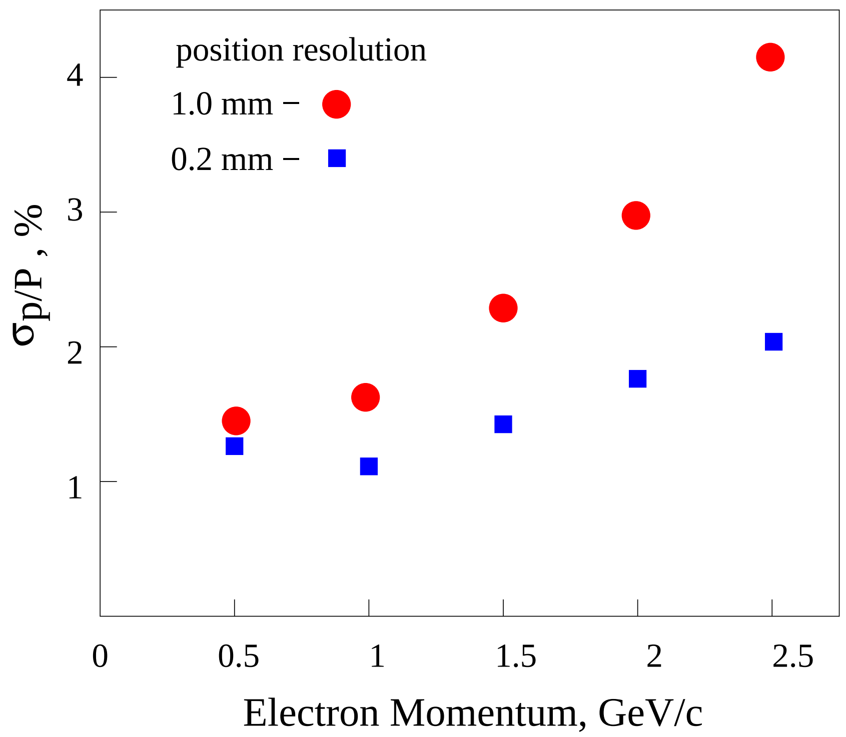

Figure 9: The momentum resolution of the Big Bite spectrometer.

momentum above 0.1 GeV/c are: positrons less than 1.0 kHz, π^+ less than 70 kHz, and protons less than 10 kHz. Therefore, the overall charge particle rate in Big Bite above 0.1 GeV/c momentum should be less than 160 kHz for the hydrogen target. Singles rates for deuterium and helium-3 target should be comparable under similar luminosity. We realize that the low energy background on the Big Bite wire chambers will likely to be the instrumentation limitation for this experiment. Compare with the background situation in E02013, this experiment has a factor of four less solid angle and a factor of 6 more luminosity in term of number of nucleons in the beam. By taking Big Bite to a large drift distance, we will have extra 1.2 meter of space before the magnet to build up heavy shielding and install a thick collimator. Further more, we plan to shield the edge area of the wire chambers to reduce chamber activities caused by low energy particles.

A background rate test of the Big Bite spectrometer is planned in Hall A later this year. Improvements on the design of the detector and shielding are very much expected. In addition, several other experiments are planning to use Big Bite before this experiment starts. Knowledge on the origin of the background will help us further reduce the low energy particle rates. Since this experiment has a relatively high coincident rates, further reduce the Big Bite solid angle is also an option.

For the left HRS at 6°, the electron singles rate in the worst case is less than 100 kHz, and positron rates are less than 1 kHz. Pion singles rates are less than 100

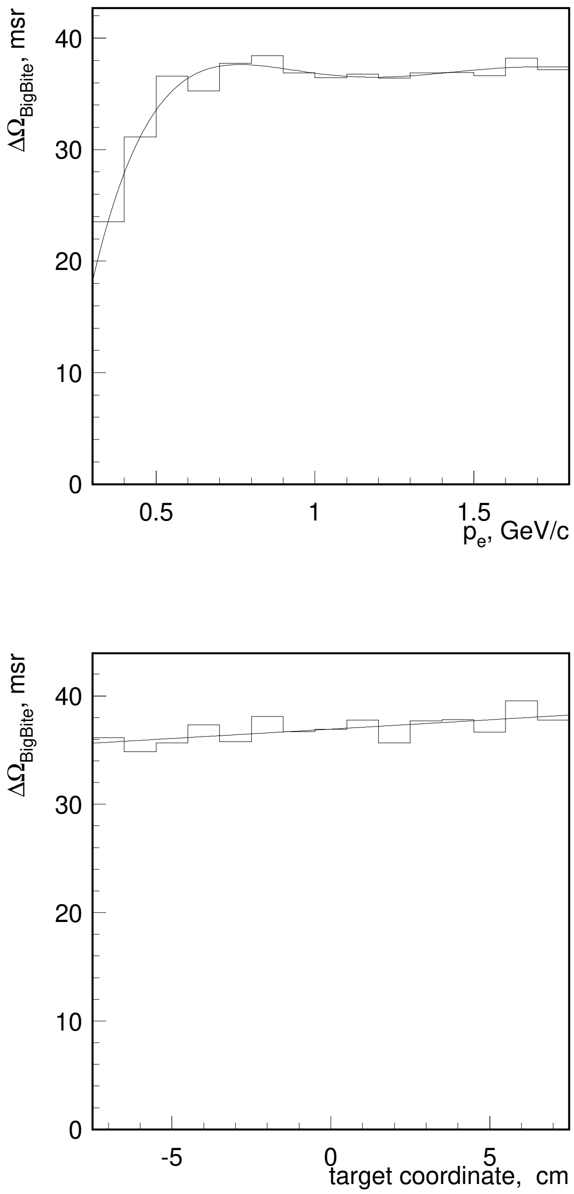

Figure 10: The Big Bite solid angle acceptance as a function of the particle momentum (top) and the interaction point along the beam (bottom).

kHz, and proton singles rates are of the order of a few kHz. The combination of the threshold gas Cherenkov and two layers of lead-glass shower counters should provide sufficient e^-/π^- and e^+/π^+ separation. Aerogel signal in combination with tracking corrected time-of-flight information could clearly separate π^+ from proton.

The accidental (e,π^+) or (e,π^-) coincident rate should be less than 100 Hz within a time window of 100 ns. The trajectory corrected time-of-flight resolution is expected to be better than 1.0 ns. Since both arms have an interaction point resolution of at least 2.0 cm along the beam, an additional accidental reduction factor of 7.5 can be achieved for a 15 cm long target. Assuming a 2.0 ns coincident time cut, the accidental rates of $(e^-\pi^-)$ or $(e^-\pi^+)$ would be at 0.3 Hz level while the overall true coincident rate will be above 3 Hz summing over six x-bins. Therefore, the signal-to-noise ratio will be higher than 10:1 in the worst case.

3 Count Rate Estimate and Beam Time Request

3.1 Coincident $(e,e'\pi)$ Cross Section Model and Rate Estimate.

The model of coincident cross sections has the following inputs:

- The inclusive (e, e′) cross sections for protons, deuteron, and helium-3.
- A parameterization of the fragmentation functions $D^+(z)$ and $D^-(z)$ as a function of Q^2.
- A model of the transverse momentum distributions of pions as fragmentation products.

The inclusive deep inelastic (e,e') cross section can be expressed in the quark parton model as:

$$\frac{d^2\sigma}{d\Omega dE'} = \frac{\alpha^2(1+(1-y)^2)}{sxy^2}\frac{E'}{m_N\nu}\sum_i e_i^2\left(q_i(x,Q^2)+\bar{q}_i(x,Q^2)\right) \tag{9}$$

where m_N is the nucleon mass, $y=\nu/E$, $s=2Em_N+m_N^2$. The quark distribution functions $q_i(x,Q^2)$ and $q_{\bar{i}}(x,Q^2)$ are taken from the CTEQ5M global fits [13]. The predicted inclusive cross sections agree with SLAC data[14] to better than 20% within the kinematic region of this proposal.

The semi-inclusive $(e,e'h)$ cross section relates to the quark fragmentation function $D_i^h(z,Q^2)$ and the total inclusive cross section σ_{tot} through:

$$\frac{1}{\sigma_{tot}}\frac{d\sigma(e,e'h)}{dz} = \frac{\sum_i e_i^2 f_i(x,Q^2)D_i^h(z,Q^2)}{\sum_i e_i^2 f_i(x,Q^2)}. \tag{10}$$

The two light quark fragmentation functions, $D^+(z,Q^2)$ and $D^-(z,Q^2)$, relate to each other approximately through [15]:

$$\frac{D^-(z,Q^2)}{D^+(z,Q^2)} = \frac{1-z}{1+z}. \tag{11}$$

The average pion fragmentation function $D^{\pi}(z,Q^2)$=1/2($D^+(z,Q^2)$ + $D^-(z,Q^2)$) was parameterized (BKK parameterization) [16] based on fits of e^+e^- annihilation data. Existing data indicated that the fragmented products follow a nearly structure less azimuthal distribution and a Gaussian-like transverse distribution. For the $p(e,e'\pi^+)X$ reaction, at the kinematic point of $\nu = 4.10$ GeV, $W^2 = 4.56$ GeV^2 and Q^2=1.20 GeV^2, Bebeck *et al.* [17] determined that the pion transverse momentum ($p_\perp$) distribution follows the form of $e^{(-Bp_\perp^2)}$ with B=8.09 $\pm$ 0.65 GeV^{-2}, corresponding to a quark transverse momentum distribution of $\sigma_{p_\perp} = 0.25$ GeV. We used this pion distribution and realistic spectrometer acceptances in a Monte Carlo simulation to estimate the count rates. We note that when a virtual photon of several GeV strikes a quark, the majority of the fragmentation products remain within a few degrees of the direction of the virtual photon. Therefore, by detecting fragmentation products along the direction of $\vec{q}$, the Hall-A HRS spectrometer provides sufficient solid angle coverage. In this proposal, the kinematics are chosen such that the direction of $\vec{q}$ always lies within the acceptance of HRS.

With a 5 μA beam on a 15 cm standard Hall-A cryogenic hydrogen/deuterium target, the luminosity is 2.0×10^{37} (nucleon) cm^{-2}s^{-1}. The HRS spectrometer with the septum magnet has an angular acceptance of $\Delta\theta_{hor} =^{+24}_{-19}$ mrad and$\Delta\theta_{ver} = \pm 50$ mrad, and a momentum acceptance of $\pm 4.5\%$ [18]. The Big Bite spectrometer will be kept in one setting throughout this experiment. It will detect charged particles over a momentum range of $0.6 \sim 1.8$ GeV/c with reasonable resolution. Because of this large momentum bite, data can be binned in six x-bins from $x = 0.11$ to $x = 0.34$. An electron detection efficiency of 90% is assumed.

To test the violation of factorization, we take five different P_π settings between 1.7 to 3.7 GeV/c. The beam time are chosen such that a sample of 25,000 coincident events could be collected for each setting in the $x = 0.19$ bin. After event selection cuts and transverse momentum (P_t) cuts, we hope to achieve 2.0% statistical accuracy on t_1 and t_2 in the $x = 0.19$ bin.

The time distribution within one setting is chosen such that the yields from hydrogen, deuterium and helium-3 targets are measured with similar relative accuracies and yields of $\pi+$ and π^- are measured with similar statistical precision.

The estimated count rates and beam time allocations for each x-bin are listed in Table 3.

We also plan to spend 42 hours on the Deuterium target and another 42 hours on the Helium-3 target. In order to keep the Big Bite detectors in a similar environment, we plan to run Deuterium and Helium-3 targets at a similar luminosity in term of the number of nucleons as the Hydrogen target such that the singles rates stay the same throughout the experiment. This implies that the liquid Deuterium target will be run at an average current of $2 \sim 3$ μA. The 10 cm Helium-3 target, operating at a temperature of 20K and a pressure of 250 psi, will be run at a beam current of 27 μA. The time sum ($T^{\pi^+} + T^{\pi^-}$) in each HRS momentum will be kept the same in Deuterium and Helium-3 runs as in the Hydrogen runs, and they will be evenly split between positive and negative HRS settings. Once nuclear corrections are

Table 3: Estimated coincident rates (in Hz) in each 0.2 GeV E'-bin for five HRS momentum settings (P_{HRS} in GeV/c) on a Hydrogen target, the average x values for each bin are listed. Beam times (in hour) under each HRS setting are listed in the right two columns. The rates are based on a 5 μA beam on a 15 cm liquid Hydrogen target. Count rates for those bins with an average $W' < 1.8$ GeV are not listed.

P_{HRS}	π^+	π^-	π^+	π^-	π^+	π^-	π^+	π^-	π^+	π^-	π^+	π^-	T^{π^+}	T^{π^-}
	$x = 0.11$		0.15		0.19		0.24		0.29		0.34		Hour	
1.70	7.0	3.6	5.8	2.9	4.6	2.2	3.6	1.7	2.7	1.2	2.0	0.9	1.4	3.0
2.20	7.7	3.2	5.9	2.4	4.5	1.7	3.4	1.2	2.5	0.9	1.7	0.6	1.5	3.9
2.70	7.6	2.5	5.6	1.7	4.0	1.2	2.9	0.8	2.0	0.5	-	-	1.6	5.7
3.20	6.9	1.7	4.7	1.1	3.2	0.7	-	-	-	-	-	-	2.0	9.8
3.70	5.7	1.0	-	-	-	-	-	-	-	-	-	-	1.9	10.8
Sum													8.4	33.2
Time on Hydrogen Target													**42**	
(Time on Deuterium Target)													(42)	
(Time on Helium-3 Target)													(42)	
Total Data Collection Time													**126**	

demonstrated to be well understood, neutron yield could be formed from combined Deuterium and Helium-3 data to enhance statistical accuracies.

The beam time request is summarized in Table 4. In addition to 126 hours of production beam time, we request 3 hours for dummy target yield check, 16 hours for Big Bite detector check and optics calibration and 3 hours for HRS magnet polarity change, 3 hours for HRS momentum changes, 3 hours for target movements and 3 hours for HRS short single arm runs. Since the planned Big Bite spectrometer and its detector package will be used in similar ways in several other Hall A experiments, some shared calibration beam time is expected to be available before this experiment starts. Additional Hall A facility development time will also be available to the Big Bite collaboration for additional calibrations and detector shakedown.

4 Expected Results

We plan to measure yield ratios rather than absolute cross sections. Most of the systematic uncertainties drop out of the ratios, such as those from acceptance and absolute beam charge. Sensitivity to instrumental effects are minimized and the absolute detection efficiencies cancel in the yield ratio. The major concern with systematic uncertainties comes from the possible bias between π^+ and π^- detection and luminosity corrections. Redundancy of the particle IDs in HRS will help to determine the detection efficiency and eliminate bias between π^+ and π^- detections. We also plan to have several HRS short single arm runs with overlapping momentum settings, therefore, local detection inefficiencies can be monitored and corrected.

Table 4: Summary of beam time request.

Item	Time (Hours)
Data Production Beam Time	3 targets $\times$ 42 = 126
Big Bite Optics and Calibration	16
Dummy Target Yield Check	3
Target Movements	3
HRS Magnet Polarity Change	3
HRS Momentum Changes	3
HRS Short Single Arm Runs	3
Total Beam Time Requested	**156 (6.5 days)**

Luminosity monitoring through beam charge and target density measurement as well as spectrometer single event rates can correct the overall luminosity to 1.0% level. The difference in luminosity determination between π^+ and π^- measurements should be less than 0.5%.

To the first order, radiative corrections will cancel in the yield ratios. However, the radiative correction differences between $(e, e'\pi^+)$ and $(e, e'\pi^-)$ reaction could introduce higher order corrections. We expect this kind of higher order radiative correction difference to be relatively small in the yield ratios. In principle, this correction can be calculated exactly in the frame work of QED.

Another issue in the interpretation of this experiment is the effects of final state interaction in $(e, e'\pi^+)$ and $(e, e'\pi^-)$ reaction. We intentionally chose pion momentum to be higher than 1.70 GeV/c for reduced $\pi - N$ scattering cross section to reduce the complications of final state interactions. We also chose to avoid the resonance region by taking W' as high as possible ($1.8 < W' < 2.6$ GeV) and observing the pions directly along the momentum transfer direction. Thus we expect the effects of final state interactions to be rather small.

There's basically very little EMC effect in this region – one is still above the shadowing region ($x < 0.1$) and below the "dip" in the EMC ratio at larger x ($x = 0.5 \sim 0.7$). In light nuclei like Deuteron or Helium-3 any effect will be correspondingly smaller ($< 1 \sim 2\%$). By comparing high precision Helium-3 and Deuteron data, effects of nuclear corrections can be checked against model calculations [19].

We will have enough data to quantify the violation of factorization to better than 2.0 % statistical accuracy on the ratios of t_1 and t_2 in the three lower x-bins, and to about $2.3 \sim 3.4\%$ level in the higher three x-bins. The expected sensitivity to t_1 and t_2 are shown in Fig 11 and Fig 12. If a reasonable z-independent behavior is reproduced as in the HERMES experiment, the yield ratios could be used to form quark distribution ratios. On the other hand, our measurements could demonstrate a transition to the factorization regime which would be very interesting in itself.

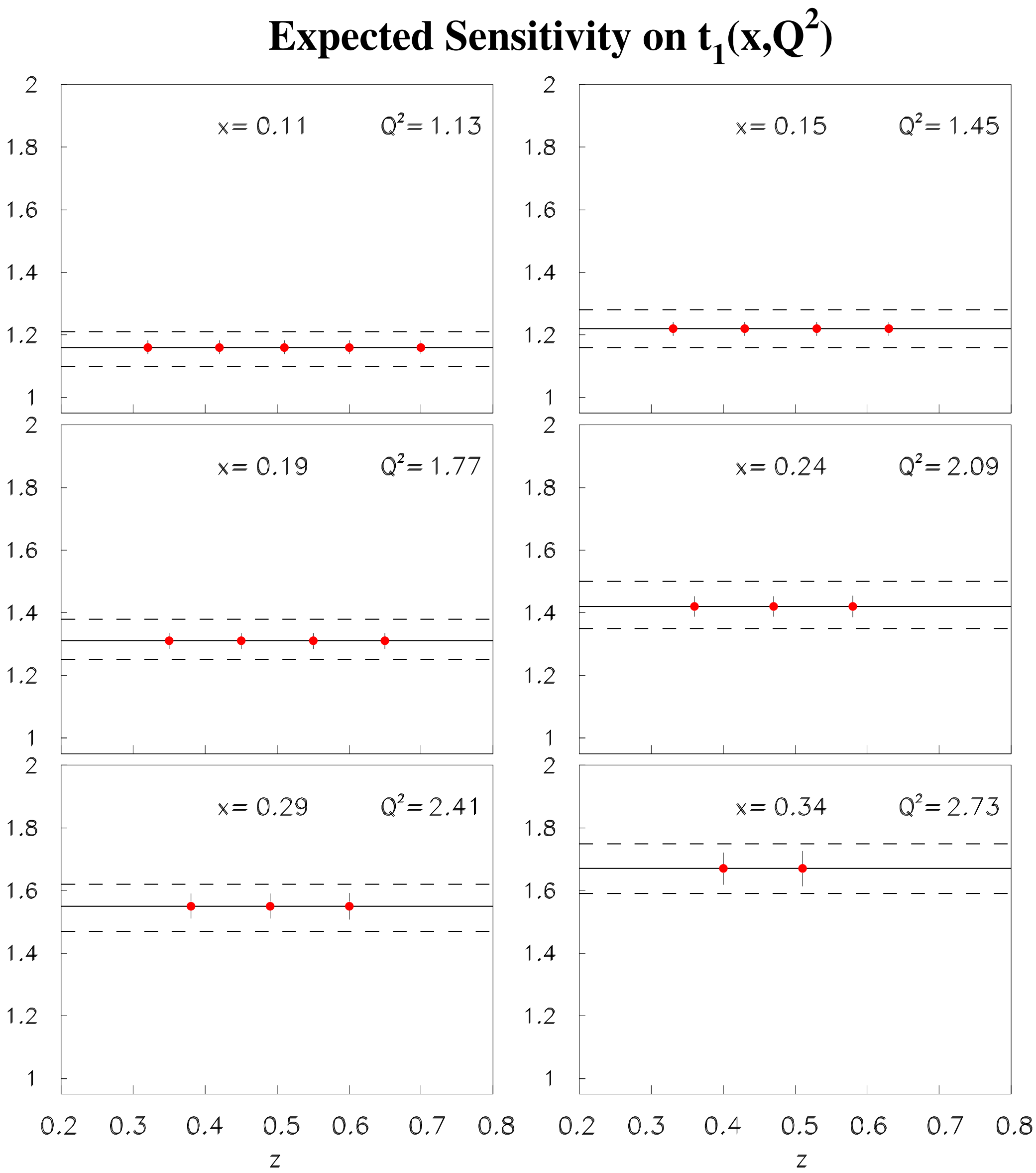

Figure 11: Expected results on $t_1(x, Q^2)$. The solid line is the expected value of $t_1(x, Q^2)$ from CTEQ5M quark distribution. The dashed lines reflect $\pm 5.0\%$ relative deviations from the factorization assumption.

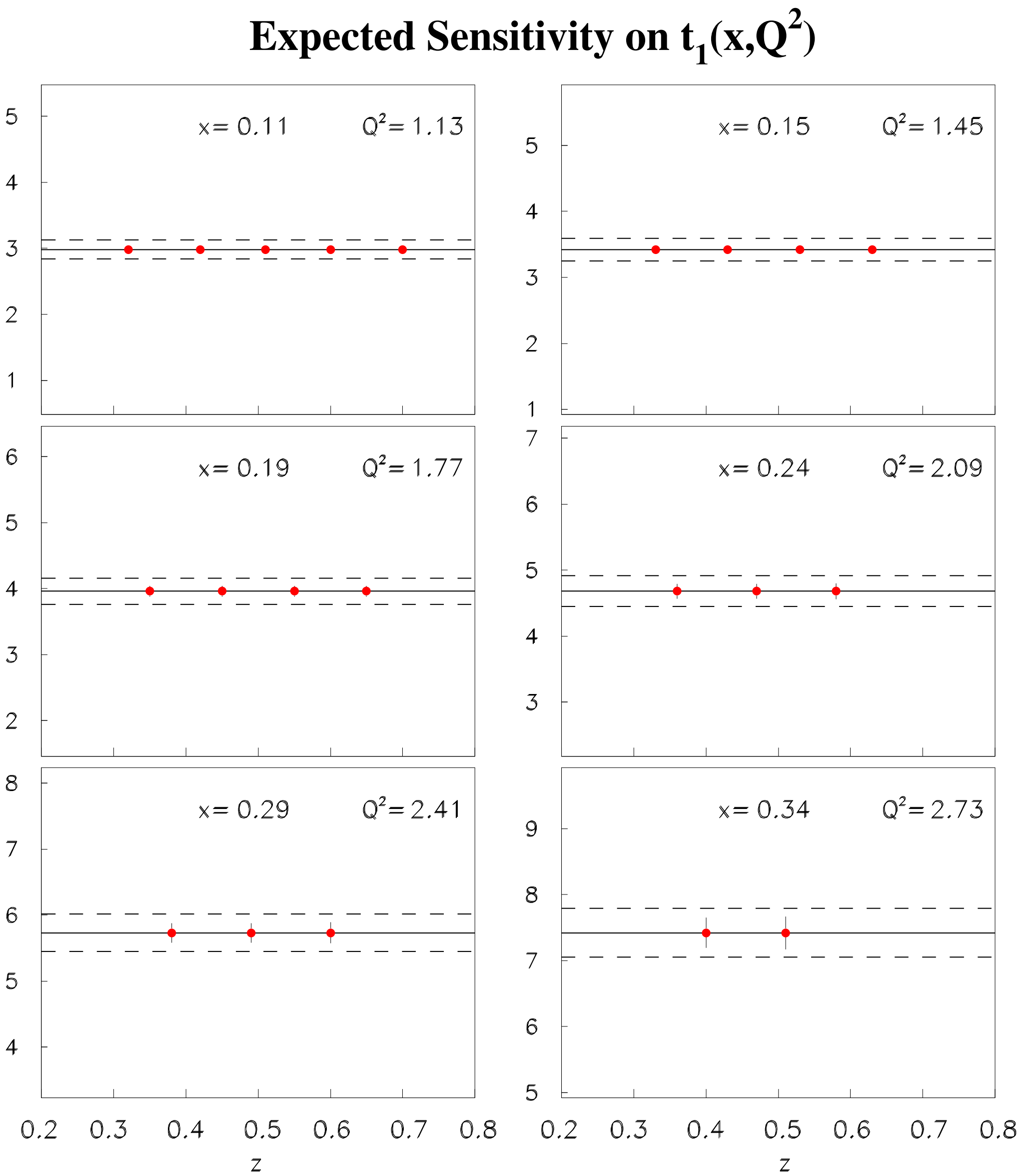

Figure 12: Expected results on $t_2(x, Q^2)$.The solid line is the expected value of $t_2(x, Q^2)$ from CTEQ5M quark distribution. The dashed lines reflect ±5.0% relative deviations from the factorization assumption.

4.1 Other possible physics by-products.

We note here that $(e, e'K^+)$ and $(e, e'K^-)$ events will also be collected in the data. Time of flight difference and PID provided by aerogel Cherenkov and RICH detector will be sufficient to separate them from $(e, e'\pi^\pm)$ events. Distributions of s-quarks could be accessed through this reaction. Although we are not planning to measure the absolute cross sections with high precision, in principle, there is no obstacle to determining the absolute detector efficiencies and spectrometer acceptances at the $\pm 5\%$ level. Therefore, inclusive (e, e') cross sections, as well as π^+/π^- production ratios can also be determined. Extraction of fragmentation functions within our acceptance are also possible with an introduction of a fragmentation model as was done in the HERMES analysis, and it will be rather interesting to compare them with parameterizations from high energy data.

5 Relation to Other Experiments

Very small forward angle access is almost impossible in Hall C. This fact makes the deep-inelastic semi-inclusive reactions, such as in the kinematics of this proposal, inaccessible to Hall C at 6 GeV energy without extensive hardware developments. We note that Hall-C approved proposal PR-00-004 (R. Ent . *et al.* PAC-18) was proposed to test "Duality in Meson Electroproduction" using the $(e, e'\pi)$ reaction in the resonance region. It was proposed to measure the absolute cross sections in order to extract fragmentation functions in the resonance region to compare with high energy data to see if there is any similarity. In contrast, this proposed experiment focuses in the deep inelastic region with $1.8 < W' < 2.6$ GeV, and measures yield ratios as a test of violation of factorization.

Existing Hall B data at 5.7 GeV has provided a large event sample in charged pion electro-production channels in the resonance region. However, because of the forward angle geometry limitation of the CLAS detector, deep inelastic semi-inclusive kinematics at high-W, high-W' and Q^2 are not accessible at the same time as they are in Hall A. In addition, combinations of π^+ and π^- yields are more complicated in Hall B since differences in tracking and detection efficiencies play a larger role in determining the yield ratios.

6 Summary

In conclusion, we will be able to make high precision measurements of π^+/π^- yield ratios on hydrogen, deuterium and helium-3 targets to quantify the violation of factorization. Jefferson Lab at 6 GeV will allow us to reach W high enough (2.5 to 3.1 GeV) while keeping W' above the resonance region such that deep inelastic semi-inclusive measurements become possible.

A total of 156 hours (6.5 days) of beam time is requested for experiment with 6 GeV unpolarized beam in Hall-A.

References

1. L. L. Frankfurt, M. I. Strikman, L. Mankiewicz, A. Schafer, E. Rondio, A. Sandacz and V. Papavassiliou, Phys. Lett. B **230**, 141 (1989); F. E. Close and R. G. Milner, Phys. Rev. D **44**, 3691 (1991).
2. R. L. Jaffe and X. Ji, Nucl. Phys. **B375**, 527 (1992).
3. J. Levelt, P.J. Mulders and A.W. Schreiber, *Phys. Lett.* B **263**, 498 (1991),
4. M. Glück, *et al.*, *Z. Phys.* C **67**, 433 (1995).
5. J. E. Belz, HERMES Collaboration., Proceedings of the Symposium of Meson and Nucleon Interactions, Vancouver, Canada, August 1997.
6. P. Geiger, Ph.D. thesis, Ruprecht-Karls-University, Heidelberg, 1998
7. W. Melnitchouk, *et al.*, *Phys. Lett.* B **435**, 420 (1998).
8. G. Cates, K. McCormick, B. Reitz and B. Wojtsekhowski, Jefferson Lab experiment E02-013: "Measurement of the Neutron Electric Form Factor G_E^n at High Q^2" (2002).
9. P. J. Mulders, hep-ph/0010199, "Current fragmentation in semi-inclusive leptoproduction".
10. T. Sloan, G. Smadja and R. Voss, *Phys Rep.* 162 (1988) 45.
11. V. Nelyubin, Big Bite Monte Carlo simulation, private communications.
12. P. Degtiarenko, private communications.
13. H. L. Lai, *et al.*, *Phys. Rev.* D **55**, 1280 (1997).
14. L. W. Whitlow, SLAC-Report-357, March (1990).
15. R. D. Field and R. P. Feynman, *Nucl. Phys.* B **136**, 1 (1978).
16. J. Binnewies, B. A. Kniehl and G. Kramer, *Phys. Rev.* D **52**, 4947 (1995).
17. C. J. Bebek, *et al.*, *Phys. Rev. Lett.* **30**, 624 (1973).
18. J. LeRose, private communication, and Hall-A Hypernuclear Collaboration, Technical Notes on Septum Magnets Design, September (1996).
19. W. Melnitchouk, *Phys. Rev.* D **59**, 14033 (1999).